Total ionization cross section for electron-hydrogen scattering using a time-dependent close-coupling method

M. S. Pindzola and F. Robicheaux
Department of Physics, Auburn University, Auburn, Alabama 36849
(Received 29 February 1996)

A time-dependent close-coupling method is combined with a time-independent distorted-wave method to calculate the electron ionization cross section for hydrogen. A second-order differencing of the time propagator for the close-coupled equations is found to be very efficient. Low partial-wave close-coupling results are added to high partial-wave distorted-wave results to yield total ionization cross sections in excellent agreement with experiment between 30- and 50-eV incident electron energy. The distorted-wave method found most suitable for the high partial waves is based on a mixture of V^N and V^{N-1} scattering potentials. [S1050-2947(96)06309-3]

PACS number(s): 34.80.Dp

I. INTRODUCTION

Electron scattering on hydrogenic targets remains a very useful testing ground for the development of new theoretical approaches [1]. Recently a time-dependent close-coupling method [2] was employed to calculate the $L=0$ and $L=1$ partial-wave cross sections for the electron ionization of hydrogen. The partial cross sections obtained from this wave-packet approach were found to be in good agreement with those obtained from a time-independent converged close-coupling method [3].

In this paper we extend the time-dependent calculations to include all $L=0$ to $L=4$ partial-wave ionization cross sections for electron scattering from hydrogen. A key factor in obtaining all the low L partial cross sections is the implementation of a second-order differencing method [4] for the time propagation of the close-coupled equations. This propagation scheme is easily an order of magnitude faster than the Taylor-series method employed in earlier calculations. The total ionization cross section for hydrogen can now be obtained by combining the $L=0$ to $L=4$ time-dependent close-coupling results with $L=5$ to $L=30$ time-independent distorted-wave results. The combined ionization cross section is found to be in excellent agreement with experiment [5] for incident electron energies between 30 and 50 eV. The wave-packet theory is reviewed in Sec. II, the ionization cross sections for hydrogen are presented in Sec. III, and a brief summary is found in Sec. IV.

II. THEORY

The time-dependent close-coupling method [2] is a wave-packet solution [6] to the same set of close-coupled partial differential equations used in time-independent electron-atom scattering theory [7–9]. For electron scattering from a one-electron target atom, the Hamiltonian (in atomic units) is given by

$$H=-\frac{1}{2}\nabla_1^2-\frac{1}{2}\nabla_2^2-\frac{Z}{r_1}-\frac{Z}{r_2}+\frac{1}{|\vec{r}_1-\vec{r}_2|}, \tag{1}$$

where the $\vec{r}_1$ and $\vec{r}_2$ are the coordinates of the two electrons and Z is the atomic number. The total wave function may be expanded in coupled spherical harmonics:

$$\Psi^{LS}(\vec{r}_1,\vec{r}_2,t)=\sum_{l_1,l_2}\frac{P^{LS}_{l_1l_2}(r_1,r_2,t)}{r_1r_2}\times\sum_{m_1,m_2}C^{l_1l_2L}_{m_1m_20}Y_{l_1m_1}(\hat{r}_1)Y_{l_2m_2}(\hat{r}_2), \tag{2}$$

where L and S are the total orbital and spin angular momentum of the system, $Y_{lm}(\hat{r})$ is a spherical harmonic, and $C^{l_1l_2l_3}_{m_1m_20}$ is a Clebsch-Gordan coefficient. From projection onto the time-dependent Schrödinger equation, we obtain the following set of time-dependent close-coupled partial differential equations for each LS symmetry:

$$i\frac{\partial P^{LS}_{l_1l_2}(r_1,r_2,t)}{\partial t}=T_{l_1l_2}(r_1,r_2)P^{LS}_{l_1l_2}(r_1,r_2,t)+\sum_{l_1',l_2'}V^{L}_{l_1l_2,l_1'l_2'}(r_1,r_2)P^{LS}_{l_1'l_2'}(r_1,r_2,t), \tag{3}$$

where

$$T_{l_1l_2}(r_1,r_2)=-\frac{1}{2}\frac{\partial^2}{\partial r_1^2}-\frac{1}{2}\frac{\partial^2}{\partial r_2^2}+\frac{l_1(l_1+1)}{2r_1^2}+\frac{l_2(l_2+1)}{2r_2^2}-\frac{Z}{r_1}-\frac{Z}{r_2}, \tag{4}$$

and the coupling operator is given by

$$V^{L}_{l_1l_2,l_1'l_2'}(r_1,r_2)=(-1)^{L+l_2+l_2'}\sqrt{(2l_1+1)(2l_1'+1)(2l_2+1)(2l_2'+1)}\times\sum_{\lambda}\frac{r_<^{\lambda}}{r_>^{\lambda+1}}\begin{pmatrix}l_1&\lambda&l_1'\\0&0&0\end{pmatrix}\begin{pmatrix}l_2&\lambda&l_2'\\0&0&0\end{pmatrix}\begin{Bmatrix}L&l_2'&l_1'\\\lambda&l_1&l_2\end{Bmatrix}. \tag{5}$$

We solve the time-dependent close-coupled equations using lattice techniques to obtain a discrete representation of

the radial wave functions and all operators on a two-dimensional grid. When finite difference methods are employed, local operators become diagonal matrices and derivative operators, such as the kinetic energy, have lattice representations in terms of banded matrices. For simplicity, all calculations discussed here implement uniform mesh spacing.

The total wave function at time $t=0$ is constructed as the antisymmetrized product of an incoming radial wave packet for one electron and the lowest energy bound stationary state of the other electron. For $L=0$, then

$$P_{00}^{0S}(r_1,r_2,t=0)=\sqrt{\tfrac{1}{2}}[g_{ks}(r_1)P_{1s}(r_2) +(-1)^S P_{1s}(r_1)g_{ks}(r_2)], \tag{6}$$

and for $L\neq 0$ and $l=L$,

$$P_{l0}^{LS}(r_1,r_2,t=0)=\sqrt{\tfrac{1}{2}}g_{kl}(r_1)P_{1s}(r_2),$$

$$P_{0l}^{LS}(r_1,r_2,t=0)=\sqrt{\tfrac{1}{2}}(-1)^S P_{1s}(r_1)g_{kl}(r_2), \tag{7}$$

where k is the linear momentum, $g_{kl}(r)$ is a radial wave packet, and $P_{1s}(r)$ is the bound radial orbital.

For a given LS symmetry, the time evolution of a single-channel partial differential equation may be given by

$$P_{l_1l_2}^{LS}(t+\Delta t)=\exp[-i\Delta t H_{l_1l_2}^{L}]P_{l_1l_2}^{LS}(t), \tag{8}$$

where

$$H_{l_1l_2}^{L}=T_{l_1l_2}+V_{l_1l_2,l_1l_2}^{L}, \tag{9}$$

and the spatial coordinates have been suppressed. Another formulation uses the symmetric relation [4]

$$P_{l_1l_2}^{LS}(t+\Delta t)-P_{l_1l_2}^{LS}(t-\Delta t) =(\exp[-i\Delta t H_{l_1l_2}^{L}]-\exp[+i\Delta t H_{l_1l_2}^{L}])P_{l_1l_2}^{LS}(t). \tag{10}$$

For a given time step Δt, many more terms in the expansion of the exponential are needed for the asymmetric relation of Eq. (8) than for the symmetric relation of Eq. (10) to preserve the norm of the wave function. For our purposes we employ the simple ''staggered leapfrog'' approximation [10]:

$$P_{l_1l_2}^{LS}(t+\Delta t)-P_{l_1l_2}^{LS}(t-\Delta t)=-2i\Delta t H_{l_1l_2}^{L}P_{l_1l_2}^{LS}(t), \tag{11}$$

involving only one Hamiltonian matrix multiplication per time step. Norm conservation is exact if we adjust the time step to be less than 1 divided by the eigenvalue with largest absolute value of the discrete Hamiltonian operator. The time evolution equations for the single-channel case can be easily generalized to handle arbitrary numbers of coupled equations. In practice, we find that the ''staggered leapfrog'' method is easily an order of magnitude faster than a direct Taylor series expansion of Eq. (8), mainly due to the vast decrease in the number of matrix-vector multiplications. We also note that all of these explicit time propagators can be easily implemented on massively parallel computers.

The total wave function at a time $t=T$ following the collision is used to calculate the spin-averaged electron-impact ionization cross section given by

$$\sigma_{\rm ion}=\frac{\pi}{4k^2}\sum_{L,S}(2L+1)(2S+1)\wp_{\rm ion}^{LS}, \tag{12}$$

where

$$\wp_{\rm ion}^{LS}=1-\sum_{nlm}\wp_{nlm}^{LS} -\sum_{nlm}\sum_{n'l'm'}|\langle\Psi^{LS}(\vec{r}_1,\vec{r}_2,T)|\phi_{n'l'm'}(\vec{r}_1)\phi_{nlm}(\vec{r}_2)\rangle|^2. \tag{13}$$

In the above equations, $\wp_{\rm ion}^{LS}$ is the probability for ionization and $\wp_{nlm}^{LS}$ is the probability of finding only one electron in a bound state $\phi_{nlm}(\vec{r})$ and the other electron in the continuum. The third term on the right-hand side of Eq. (13) is the probability of finding both electrons in bound states. The bound-state probabilities are given by

$$\begin{aligned}\wp_{nlm}^{LS}=&\int d\vec{r}_1|\langle\Psi^{LS}(\vec{r}_1,\vec{r}_2,T)|\phi_{nlm}(\vec{r}_2)\rangle|^2\\ &-\sum_{n'l'm'}|\langle\Psi^{LS}(\vec{r}_1,\vec{r}_2,T)|\phi_{n'l'm'}(\vec{r}_1)\phi_{nlm}(\vec{r}_2)\rangle|^2\\ &+\int d\vec{r}_2|\langle\Psi^{LS}(\vec{r}_1,\vec{r}_2,T)|\phi_{nlm}(\vec{r}_1)\rangle|^2\\ &-\sum_{n'l'm'}|\langle\Psi^{LS}(\vec{r}_1,\vec{r}_2,T)|\phi_{nlm}(\vec{r}_1)\phi_{n'l'm'}(\vec{r}_2)\rangle|^2.\end{aligned} \tag{14}$$

III. CROSS-SECTION RESULTS

The time-dependent close-coupled partial differential equations of Eqs. (3)–(5) were solved for electron scattering from a hydrogen atom with incident energies in the range from 30–50 eV. For these energies the repulsive interaction between the electrons has a sufficiently short-range nature so that moderate lattice sizes may be employed. For near threshold ionization, however, a large numerical lattice would be needed. After several test calculations, we settled on a 200×200 lattice with each radial direction from 0 to 40 spanned by a uniform mesh with spacing $\Delta r=0.2$. As previously reported [2], the ground state of hydrogen on this lat-

TABLE I. Partial-wave channel quantum numbers.

Angular momentum L	Channels	Angular momenta (l_1,l_2)
0	3	$s^2+p^2+d^2$
1	6	$sp+ps+pd+dp+df+fd$
2	6	$sd+ds+p^2+pf+fp+d^2$
3	8	$sf+fs+pd+dp+pg+gp+df+fd$
4	8	$sg+gs+pf+fp+ph+hp+d^2+f^2$

TABLE II. Partial ionization cross sections (10^{-18} cm^2).

Angular momentum L	Method	Incident energy 30 eV	40 eV	50 eV
0	TDCC	3.09	2.85	2.52
	DW1	6.49	5.19	4.02
	DW2	4.57	3.74	2.99
1	TDCC	6.36	6.02	5.41
	DW1	10.4	8.70	7.11
	DW2	8.76	7.38	6.09
2	TDCC	11.9	10.8	9.34
	DW1	18.1	16.0	13.0
	DW2	17.8	14.3	11.4
3	TDCC	11.5	11.7	10.8
	DW1	13.1	14.4	13.3
	DW2	19.1	16.8	14.1
4	TDCC	7.95	9.60	9.85
	DW1	7.99	10.7	11.1
	DW2	14.7	15.0	13.6

tice is good to 1.0%. The initial wave packets of Eqs. (6) and (7) were propagated from $t=0$ to $t=T=20-25$. The ionization probability of Eq. (13) was monitored as a function of time and was well converged for all partial waves by $t=T$. The time step for a norm-conserving time propagation ranged from $\Delta t=0.010-0.001$. The number of coupled channels needed to converge a particular partial ionization cross section varied according to total angular momentum. In Table I we list the channel quantum numbers (l_1,l_2) used in the largest close-coupling calculation for each angular momentum (L).

Electron-impact partial ionization cross sections for $L=0-4$ scattering from hydrogen are presented in Table II. The time-dependent close-coupling (TDCC) results are compared with two different time-independent distorted-wave calculations. Both distorted-wave methods are based on a triple partial-wave expansion of the first-order perturbation-theory scattering amplitude, including both direct and exchange terms. The first distorted-wave method (DW1) requires the incident and scattered electrons to be calculated in a V^N potential, while the bound and ejected electrons are calculated in a V^{N-1} potential [11]. The second distorted-wave method (DW2) requires that all electrons be calculated in a V^{N-1} potential [12]. A more thorough exposition on the two distorted-wave methods is found in a recent paper on the electron ionization of the iron atom [13].

TABLE III. Total ionization cross sections (10^{-18} cm^2).

Method	Incident energy 30 eV	40 eV	50 eV
DW1(0→30)	65.5	74.1	74.3
TDCC(0)+DW1(1→30)	62.1	71.8	72.8
TDCC(0→1)+DW1(2→30)	58.1	69.1	71.1
TDCC(0→2)+DW1(3→30)	51.9	63.9	67.5
TDCC(0→3)+DW1(4→30)	50.3	61.2	65.0
TDCC(0→4)+DW1(5→30)	50.2	60.1	63.8

TABLE IV. Total ionization cross sections (10^{-18} cm^2).

Method	Incident energy 30 eV	40 eV	50 eV
DW2(0→30)	85.4	87.6	83.8
TDCC(0)+DW2(1→30)	83.9	86.7	83.3
TDCC(0→1)+DW2(2→30)	81.5	85.4	82.6
TDCC(0→2)+DW2(3→30)	75.6	81.8	80.6
TDCC(0→3)+DW2(4→30)	67.9	76.7	77.3
TDCC(0→4)+DW2(5→30)	61.1	71.3	73.6

As reported previously [2], the second distorted-wave method is in better agreement with the more exact TDCC method for $L=0$ and $L=1$ scattering. The situation reverses, however, for the higher partial-wave cross sections. For $L=3$ and $L=4$ scattering, the first distorted-wave method is in better agreement with the more exact TDCC method. For high angular momentum scattering the first distorted-wave method is physically more appealing. Due to the high-angular-momentum barrier, a direct scattering mechanism should begin to dominate. In other words, the incoming electron cannot easily penetrate into the core region. The scattering electron always experiences a fully screened V^N potential. The ejected electron is never screened by a high-angular-momentum incoming electron; thus, it experiences a potential that is only screened by the remaining core electrons giving a V^{N-1} potential.

The superiority of the DW1 method over the DW2 method for high angular momenta is further illustrated in Tables III and IV. Starting with pure distorted-wave results for the total ionization cross section at three incident energies, we successively substitute the more exact TDCC results for the low partial-wave cross sections. By $L=4$ the TDCC plus DW1 results have converged the total ionization cross section. On the other hand, by $L=4$ the TDCC plus DW2 results have still not converged, and most likely will only converge when the TDCC results have completely replaced the DW2 results.

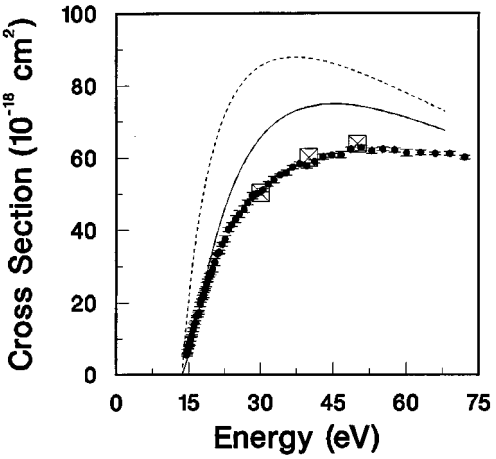

FIG. 1. Total electron-impact ionization cross section for hydrogen. Large crossed boxes, hybrid TDCC plus DW1 method; solid curve, DW1 method; dashed curve, DW2 method; solid circles, experimental measurements [5].

The total ionization cross section for hydrogen calculated using the hybrid TDCC plus DW1 method is compared with experiment [5] in Fig. 1. The excellent agreement between the hybrid theory and experiment rivals that obtained between the recently reported time-independent converged close-coupling theory [3] and the same experiment. The pure DW1 and DW2 results for the total ionization cross section are also included in Fig. 1.

IV. SUMMARY

The recently formulated time-dependent close-coupling method [2] is used to calculate $L=0$ to $L=4$ partial ionization cross sections for electron scattering from hydrogen. The replacement of the previous Taylor-series time propagator with a second-order differencing scheme was crucial to the timely completion of the calculations. Comparison of the TDCC results with time-independent distorted-wave results reveals that the choice of mixed V^N and V^{N-1} potentials for the distorted waves is superior at high angular momentum to the choice of a V^{N-1} potential alone. A hybrid close-coupling and distorted-wave method was then found to converge the total ionization cross section at three different energies and to give results in excellent agreement with experiment.

In the future we hope to apply the time-dependent close-coupling method, through the use of core potentials and a single active electron approximation, to the calculation of low L partial ionization cross sections for a variety of atomic configurations. Combining the wave-packet approach for low L with the perturbative distorted-wave approach for high L promises to yield a hybrid method capable of generating accurate total ionization cross sections for many complex atoms.

ACKNOWLEDGMENTS

In this work M.S.P. was supported in part by an NSF Grant (No. NSF-PHY-9122199) with Auburn University and F.R. was supported in part by an NSF Young Investigator Grant (No. NSF-PHY-9457903) with Auburn University. Computational work was carried out at the National Energy Research Supercomputer Center in Livermore, California.

[1] I. Bray and A. T. Stelbovics, Adv. At. Mol. Opt. Phys. **35**, 209 (1995).
[2] M. S. Pindzola and D. R. Schultz, Phys. Rev. A **53**, 1525 (1996).
[3] I. Bray and A. T. Stelbovics, Phys. Rev. Lett. **70**, 746 (1993).
[4] C. Leforestier, R. H. Bisseling, C. Cerjan, M. D. Feit, R. Friesner, A. Guldberg, A. Hammerich, G. Jolicard, W. Karrlein, H. D. Meyer, N. Lipkin, O. Roncero, and R. Kosloff, J. Comput. Phys. **94**, 59 (1991).
[5] M. B. Shah, D. S. Elliot, and H. B. Gilbody, J. Phys. B **20**, 3501 (1987).
[6] C. Bottcher, Adv. At. Mol. Phys. **20**, 241 (1985).
[7] A. Temkin, Phys. Rev. **126**, 130 (1962).
[8] J. Shertzer and J. Botero, Phys. Rev. A **49**, 3673 (1994).
[9] Y. D. Wang and J. Callaway, Phys. Rev. A **50**, 2327 (1994).
[10] W. H. Press, S. A. Teukolsky, W. T. Vetterling, and B. P. Flannery, *Numerical Recipes* (Cambridge University Press, New York, 1992), p. 833.
[11] S. M. Younger, Phys. Rev. A **22**, 111 (1980).
[12] J. H. Macek and J. Botero, Phys. Rev. A **45**, R8 (1992).
[13] M. S. Pindzola, D. C. Griffin, and J. H. Macek, Phys. Rev. A **51**, 2186 (1995).